The polymorphism rs944289 predisposes to papillary thyroid carcinoma through a large intergenic noncoding RNA gene of tumor suppressor type

Jaroslaw Jendrzejewski[a], Huiling He[a], Hanna S. Radomska[a], Wei Li[a], Jerneja Tomsic[a], Sandya Liyanarachchi[a], Ramana V. Davuluri[b], Rebecca Nagy[a], and Albert de la Chapelle[a,1]

[a]Human Cancer Genetics Program, Comprehensive Cancer Center, The Ohio State University, Columbus, OH 43210; and [b]Molecular and Cellular Oncogenesis Program, Center for Systems and Computational Biology, The Wistar Institute, Philadelphia, PA 19104

Contributed by Albert de la Chapelle, April 4, 2012 (sent for review February 20, 2012)

A genome-wide association study of papillary thyroid carcinoma (PTC) pinpointed two independent SNPs (rs944289 and rs965513) located in regions containing no annotated genes (14q13.3 and 9q22.33, respectively). Here, we describe a unique, long, intergenic, noncoding RNA gene (lincRNA) named *Papillary Thyroid Carcinoma Susceptibility Candidate 3* (*PTCSC3*) located 3.2 kb downstream of rs944289 at 14q.13.3 and the expression of which is strictly thyroid specific. By quantitative PCR, *PTCSC3* expression was strongly down-regulated ($P = 2.84 \times 10^{-14}$) in thyroid tumor tissue of 46 PTC patients and the risk allele (T) was associated with the strongest suppression (genotype [TT] ($n = 21$) vs. [CT] ($n = 19$), $P = 0.004$). In adjacent unaffected thyroid tissue, the genotype [TT] was associated with up-regulation of *PTCSC3* ([TT] ($n = 21$) vs. [CT] ($n = 19$), $P = 0.034$). The SNP rs944289 was located in a binding site for the CCAAT/enhancer binding proteins (C/EBP) α and β. The risk allele destroyed the binding site in silico. Both C/EBPα and C/EBPβ activated the *PTCSC3* promoter in reporter assays ($P = 0.0009$ and $P = 0.0014$, respectively) and the risk allele reduced the activation compared with the nonrisk allele (C) ($P = 0.026$ and $P = 0.048$, respectively). Restoration of *PTCSC3* expression in PTC cell line cells (TPC-1 and BCPAP) inhibited cell growth ($P = 0.002$ and $P = 0.019$, respectively) and affected the expression of genes involved in DNA replication, recombination and repair, cellular movement, tumor morphology, and cell death. Our data suggest that SNP rs944289 predisposes to PTC through a previously uncharacterized, long intergenic noncoding RNA gene (*PTCSC3*) that has the characteristics of a tumor suppressor.

germline variant | transcriptional regulation | tissue specific expression

Papillary thyroid carcinoma (PTC) accounts for ~85% of all thyroid carcinomas, with some 56,000 new cases estimated in the United States in 2012 (http://www.cancer.gov/cancertopics/types/thyroid). Contrary to many other cancers, its incidence is increasing (1, 2). Although the etiology of this cancer is not well characterized, it clearly is influenced by both genetic and environmental factors. Among the latter, ionizing radiation, especially exposure to fallout of radioactive iodine isotopes in childhood, strongly predisposes to PTC (3). On the other hand, genetic predisposition plays a major role, as evidenced by case-control studies. According to the largest of such studies published to date, the family risk ratio of PTC in first-degree relatives of a PTC proband is as high as 8–12, being the highest of all cancers (4–6). Some 5–10% of probands with PTC have at least one first- or second-degree relative with PTC (7, 8). However, remarkably, large families with multiple cases of PTC are rare and often do not display Mendelian inheritance. These facts suggest that the genetic predisposition is not caused by typical high-penetrance genes. Instead, low penetrance genes are likely, perhaps acting in concert with each other and/or with environmental factors (9). Such genes are not amenable to detection by linkage analysis but can be found by association analysis in large datasets (10). Until now, three genome-wide association studies (GWAS) have addressed the predisposition to PTC (11–13). Gudmundsson et al. (11) studied Icelandic PTC patients and controls, followed by validation in Spanish and US cases and controls. Two SNPs that showed highly significant association with PTC were detected (rs965513 and rs944289). The variants were located in 9q22.33 and 14q13.3, respectively, and have been confirmed by other research groups (14, 15). As both SNPs were located in gene-poor regions, no immediate candidate genes presented themselves as being affected by or associated with the risk alleles of the SNPs. In this paper, we describe experiments aimed at determining by what mechanism the SNP in 14q13.3 (rs944289) causes predisposition to PTC. We interpret our findings to suggest that a previously uncharacterized RNA gene named *Papillary Thyroid Carcinoma Susceptibility Candidate 3* (*PTCSC3*) is involved in the predisposition.

Results

Potential Candidate Genes in the 14q13.3 Region. The region containing rs944289 appeared to contain no recognized genes. Those closest to the SNP were the *Breast Cancer Metastasis-Supressor 1-Like* gene (*BRMS1L*, 308 kb centromeric) and *MAP3K12 binding inhibitory protein 1* gene (*MBIP*, 119 kb telomeric), respectively. A nearby thyroid-associated gene is *NK2 homeobox 1* (*NKX2-1*), also known as *Thyroid Transcription Factor 1* (*TTF-1*), located 337 kb telomeric of rs944289 (Fig. S1). We performed an in silico search for evidence of potential candidate genes such as Expressed Sequence Tags (ESTs) ascertained in close vicinity (~40 kb) of rs944289. We found several ESTs: CB987890, BI004592, DN993271, AA921750, AA632637, AW341561, CV391331, and AW899174. The data from the EST database (http://www.ncbi.nlm.nih.gov/dbEST/) revealed that CB987890 was derived from a pool of glandular tissues including thyroid tissue, and we confirmed that it is expressed in thyroid (Fig. 1 and Fig. S3). This potential candidate gene is located 3.2 kb downstream of rs944289 and consists of 4 exons with a total length of 0.8 kb (Fig. S2). CB987890 is located within a 40-kb linkage disequilibrium (LD) block also containing rs944289 (Fig. S2).

Author contributions: J.J., H.H., and A.d.l.C. designed research; J.J. and H.R. performed research; W.L. and R.N. contributed new reagents/analytic tools; J.J., H.H., H.R., J.T., S.L., R.V.D., and A.d.l.C. analyzed data; S.L. conducted the statistical analysis; R.V.D. performed the bioinformatic analysis; R.N. collected and characterized samples analyzed in the study; and J.J. and A.d.l.C. wrote the paper.

The authors declare no conflict of interest.

Data deposition: The sequence reported in this paper has been deposited in the GenBank database [accession no. JN689234 (PTCSC3)] and the microarray expression data have been deposited in the Gene Expression Omnibus (GEO) database, www.ncbi.nlm.nih.gov/geo (accession no. GSE32195).

[1]To whom correspondence should be addressed. E-mail: albert.delachapelle@osumc.edu.

This article contains supporting information online at www.pnas.org/lookup/suppl/doi:10.1073/pnas.1205654109/-/DCSupplemental.

www.pnas.org/cgi/doi/10.1073/pnas.1205654109

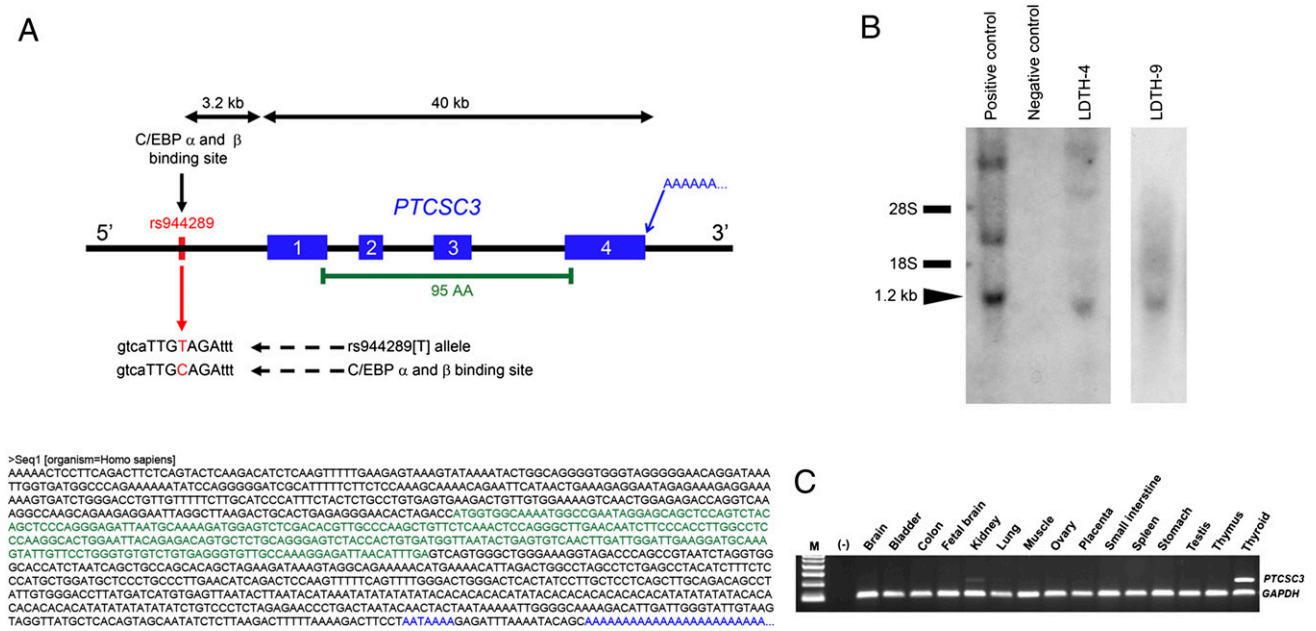

Fig. 1. Structure of *PTCSC3* with promoter region. (*A*) *PTCSC3* consists of four exons spanning more than 40 kb of genomic DNA. It contains an ORF predicting a 95-amino acid peptide starting in exon 1 and ending in exon 4. The SNP rs944289 is located 3.2 kb upstream of exon 1; rs944289 is located within a C/EBPα and C/EBPβ transcription factor binding site, and the risk allele destroys it (in silico). The full transcript sequence of *PTCSC3* (1154 bp) is shown. The ORF is marked in green, and the polyA tail signal sequence (AATAAA) and polyA tail are marked in blue. (*B*) Northern blot analysis using a *PTCSC3*-specific probe shows a ~1.2-kb band in thyroid RNA (LDTH-4, LDTH-9) and in 293T cells transfected with an expression vector harboring *PTCSC3* (Positive control) but not in the 293T cell line RNA (Negative control). (*C*) Tissue-specific expression of *PTCSC3* assessed by RT-PCR shows that *PTCSC3* is highly expressed in thyroid and very weakly in kidney tissue. *GAPDH* expression serves as a control.

Structure of the Candidate Gene. To establish the full structure of CB987890, we performed 5′ and 3′ RNA Ligase Mediated Rapid Amplification of cDNA Ends (RLM-RACE). No additional exons or isoforms were detected. Exons 1 (at the 5′ end) and 4 (at the 3′ end) were expanded by 183 bp and 192 bp, respectively. The total length of the gene is 1154 bp. We named this unique gene *Papillary Thyroid Carcinoma Susceptibility Candidate 3* (*PTCSC3*). *PTCSC3* has a potential open reading frame (ORF) predicting 95 amino acids starting in exon 1 and ending in exon 4. A single polyA signal sequence (AATAAA) was detected 18 bp before a polyA tail (Fig. 1). To confirm the size of *PTCSC3* obtained by RACE, we performed a Northern blot using RNA from 293T cells (no endogenous expression of *PTCSC3*; negative control), 293T cells transfected with *PTCSC3* expression construct (positive control) and from thyroid tissue. As shown in Fig. 1 a band around 1.2 kb was observed in the thyroid samples supporting our findings from RACE.

***PTCSC3* Is Likely a Noncoding RNA Gene.** To define the putative function of *PTCSC3* we performed computational analysis by integrating with the current genome annotations available at UCSC Genome Browser (16). We found that although the sequence of exon 1 is unique in the genome, exons 2, 3, and 4 are located within repetitive elements. Exons 2 and 3 completely overlap with LINEs (Family L1) and SINEs (Family Alu), respectively, ~75% of exon 4 overlaps with LTR repetitive elements (Family ERVL), suggesting that these exons were produced by retrotransposable elements. The genes that contain mobile genetic elements such as transposons or retrotransposons are usually noncoding RNA genes despite having sometimes short ORFs (17, 18).

***PTCSC3* Expression Is Highly Thyroid Specific.** To test whether the *PTCSC3* gene is expressed in other tissues than thyroid, we performed RT-PCR using RNA obtained from multiple tissues. Importantly, the *PTCSC3* is almost uniquely expressed in thyroid tissue with very low expression additionally in kidney tissue (Fig. 1).

***PTCSC3* Expression Is Down-Regulated in Tumor Tissue.** We analyzed *PTCSC3* expression in paired, adjacent, unaffected (PTC-N) and tumor (PTC-T) thyroid tissue samples from 46 patients by real-time PCR (Fig. 2). The *PTCSC3* RNA level was strongly or moderately down-regulated in tumor tissue compared with unaffected thyroid tissue in all of the tested pairs ($P = 2.84 \times 10^{-14}$). We also analyzed the expression of *PTCSC3* in six thyroid cancer cell lines (C643, FTC133, SW1736, TPC-1, BCPAP, KTC-1) as shown in Fig. S3 and no expression was detected in any of them.

SNP Risk Allele [T] Is Associated with Dysregulation of *PTCSC3* Expression. To assess the impact of the risk allele on suppression of *PTCSC3,* we analyzed fold changes in expression between tumor and unaffected thyroid tissue. The rs944289[T] allele was associated with stronger down-regulation of *PTCSC3* when [TT] homozygotes ($n = 21$) were compared with heterozygous [CT] patients ($n = 19$) ($P = 0.004$), but in the comparison with the few available homozygous [CC] subjects ($n = 6$) the difference did not reach statistical significance ($P = 0.110$; Fig. 2 and Fig. S4). Interestingly, in adjacent unaffected thyroid tissue *PTCSC3* expression was slightly higher in [TT] homozygotes than in [CT] heterozygotes ($P = 0.034$) (Fig. S4).

C/EBPα and C/EBPβ Regulate Transcriptional Activity of the *PTCSC3* Promoter. Computational analysis revealed the presence of a binding site for CCAAT/enhancer binding protein (C/EBP) α and β overlapping with rs944289. The SNP is located within the conserved part of the binding site (Fig. 1). We used an electrophoresis mobility shift assay (EMSA) to determine whether the binding of the C/EBP proteins to the position of rs944289 occurs in vitro. A [α-P^{32}]-dCTP radiolabeled (by Klenow) probe containing the rs944289[C] allele was used, together with

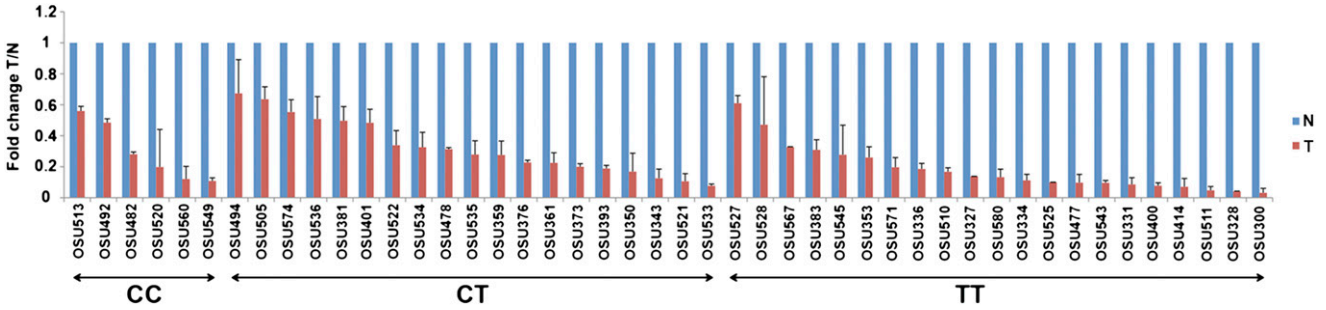

Fig. 2. Quantitative RT-PCR of *PTCSC3* expression in paired samples of unaffected tissue and PTC tumor (n = 46). N, nonaffected tissue; T, tumor tissue. Shown are values from tumor normalized against values from the corresponding unaffected tissue. Samples arranged by SNP rs944289 genotypes (CC, n = 6; CT, n = 19; TT, n = 21; CC vs. CT, P = 0.687; CC vs. TT, P = 0.110; CT vs. TT, P = 0.004).

a nuclear extract from 293T cells transfected 24 h before the nuclear extraction with empty vector (pcDNA3), p42 C/EBPα, p30 C/EBPα or C/EBPβ expression constructs. As shown in Fig. 3, p42 C/EBPα and C/EBPβ bind strongly to the site, whereas the binding of p30 C/EBPα is weaker. The specificity of C/EBPs binding was confirmed either by lack of the shift in the presence of the nuclear extract from control (pcDNA3) and by the super shift (or an abrogation of the bands) when specific antibodies against the C/EBP proteins were used. To investigate the effect of C/EBPα and C/EBPβ on the promoter activity, COS-7 cells were transfected with an expression vector harboring cDNA of C/EBPα (p30 and p42 isoforms) or C/EBPβ together with the reporter construct containing the promoter region of the *PTCSC3* with the rs944289[T] or rs944289[C] allele (Fig. 3). We observed an increase in the relative luciferase activity by both p42 C/EBPα and C/EBPβ (C allele: P = 0.0009 and P = 0.0014, respectively; T allele: P = 0.0019 and P = 0.0048, respectively) but not for p30 C/EBPα (P = 0.107 and P = 0.327 for C and T allele, respectively). The risk allele (T) decreased the *PTCSC3* promoter activity compared with nonrisk allele (C) for both p42 C/EBPα and C/EBPβ (P = 0.026 and P = 0.048, respectively).

No Germline or Somatic Mutations Were Observed in the *PTCSC3* Gene. We searched for previously undefined variants in the gene by cDNA Sanger sequencing of *PTCSC3* in 33 PTC normal/tumor tissue pairs. No mutations or new polymorphisms were found.

***PTCSC3* Inhibits Cell Growth and Affects the Expression of Genes Involved in DNA Replication, Recombination, and Repair.** In an attempt to define the biological role of *PTCSC3,* we transiently transfected TPC-1 and BCPAP cells (papillary thyroid carcinoma cell lines which completely lack expression of *PTCSC3*) with a *PTCSC3* expression construct or an empty vector (pcDNA3) as a control. The transfected cells displayed slower growth than the controls transfected with empty vector (TPC-1: P = 0.039 and P = 0.002 at 48 h and 72 h after transfection, respectively; BCPAP: P = 0.005, P = 0.008 and P = 0.019 at 24 h, 48 h, and 72 h after transfection, respectively) (Fig. S5). To assess the effect of

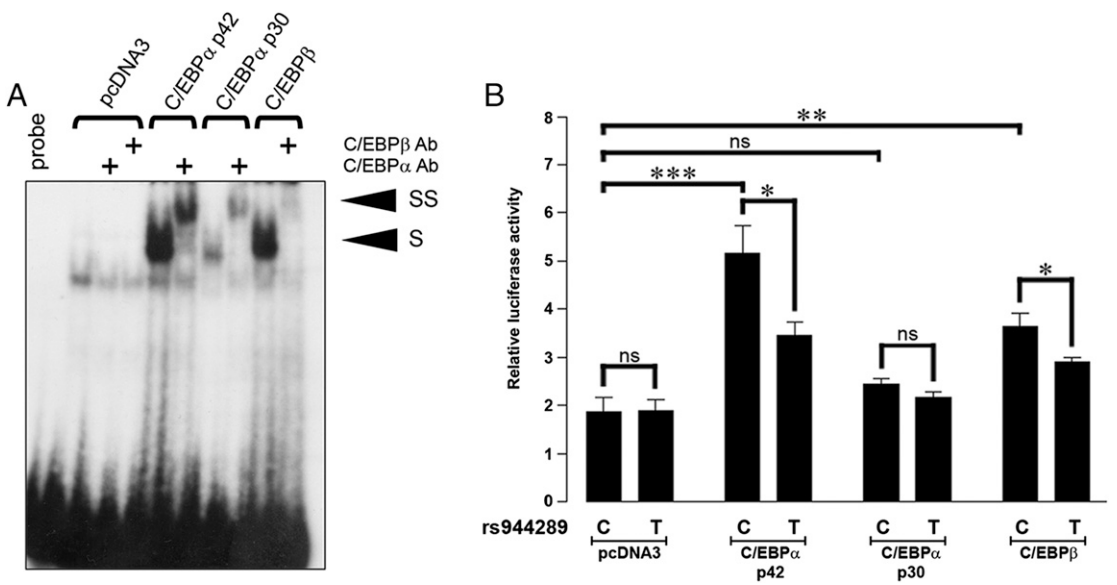

Fig. 3. Transcriptional activity of the *PTCSC3* promoter. (*A*) Electrophoretic mobility shift assay analysis of binding of C/EBP transcription factors to the rs944289 site. C/EBPα (p30 and p42 isoforms) and C/EBPβ bind to the rs944289[C] allele site as demonstrated by a shift (S) in the presence of nuclear extract from 293T cells transfected with C/EBPα (p30 or p42) and C/EBPβ constructs but not when cells were transfected with empty vector (pcDNA3). Specificity of the binding complex was confirmed by super shifts (SS) with anti-C/EBPα and anti-C/EBPβ antibodies. (*B*) Dual luciferase assay in COS-7 cells cotransfected with reporters containing *PTCSC3* promoter having either the C or T allele of the SNP sequence and C/EBPα or C/EBPβ expression vectors or empty vector. The p42 C/EBPα and C/EBPβ transcription factors stimulate transcription (C allele: P = 0.0009 and P = 0.0014, respectively; T allele: P = 0.0019 and P = 0.0048, respectively); the C allele being more active than the risk allele (T) (P = 0.026 and P = 0.048, respectively). Results are mean ± SEM of six independent experiments. *P < 0.05; **P = 0.01–0.001; ***P < 0.001; ns, not significant.

ectopically expressed *PTCSC3* on other genes we transfected TPC-1 cells (as described above) and analyzed gene expression 24 h posttransfection by Agilent SurePrint G3 Human GE8 × 60K array. The data were filtered by using volcano plot ($P < 0.05$, fold change >1.5×) to create a list of genes dysregulated by *PTCSC3* (total $n = 467$; up-regulated $n = 229$ (49%); down-regulated $n = 238$ (51%). We used Ingenuity Pathway Analysis (IPA) software to establish molecular networks and canonical pathways affected by the *PTCSC3* gene. The top three molecular networks with the highest score were as follows: Network-1: DNA Replication, Recombination, and Repair, Gene Expression, Amino Acid Metabolism (score = 45; Fig. S6); Network-2: Cellular Movement, Tumor Morphology, Cell Death (score = 40; Fig. S6); Network-3: Cellular Assembly and Organization, Cellular Function and Maintenance, Tissue Morphology (score = 39; Fig. S6). The most significant canonical pathways recognized by the IPA are presented in Table S1.

Discussion

According to a recent review, GWAS studies have already uncovered 5864 SNPs or similar markers associated with various traits (http://www.genome.gov/gwastudies/); however progress in elucidating the underlying mechanisms has turned out to be slow. Only a small number of GWAS findings have been fully interpreted (19). It is becoming increasingly clear that disease-related SNPs found by GWAS often reside outside of genes or even in regions poor in genes (also known as "gene deserts"). By way of linkage disequilibrium, these SNPs may act as surrogates for a causative genomic change within a nearby gene (20). Empirically, so far this expectation has rarely been fulfilled. Instead, a few observations point to the involvement of previously unidentified transcripts from "gene-poor" regions (21). With the availability of large-scale RNA sequencing, it is now beginning to appear that such transcripts are ubiquitous, often tissue specific, and constitute novel classes of long intergenic noncoding RNA genes (lincRNAs) (22, 23). These likely act as regulators of other genes, as has long been predicted based on experimental evidence (24–26). Our findings regarding the SNP in chromosome 14q13.3 would seem to pinpoint a prototype noncoding regulatory RNA gene. The suppression of *PTCSC3* in thyroid tumor tissue of PTC patients and the lack of its expression in PTC cell line cells that show features of poorly differentiated thyroid cancer (27) suggest that *PTCSC3* expression is lost when the normal thyroid tissue de-differentiates into cancer. Our data demonstrate that restoration of *PTCSC3* expression in TPC-1 and BCPAP cells inhibits cell growth suggesting that *PTCSC3* has tumor suppressor properties. The mechanism by which *PTCSC3* suppresses cell growth remains unknown. Our data from gene expression arrays indicated genes of major interest to PTC which might be potential targets of *PTCSC3* (e.g., *AKT*, *PI3K*, *USF2*, *RHOB;* Fig. S6) and several that have been linked with PTC (*MOAP1*, *PLK1*, *HSP90*, *PTMA*, *S100A4*, *GDF15*, *MYD88,* and *APC;* Fig. S6). Interestingly, the up-regulation of *PTCSC3* in unaffected thyroid tissue and stronger suppression in tumor tissue of homozygous [TT] patients compared with heterozygotes might suggest that the role of *PTCSC3* in the predisposition to PTC is more complex and that this lincRNA might act either as a tumor suppressor or as an oncogene, e.g., the overexpression of *PTCSC3* may support the transformation process by dysregulation of its target genes. The pronounced down-regulation of *PTCSC3* in tumor tissue likely affects other target genes of importance for tumorigenesis. The dual nature of some genes is well recognized (28, 29), but much more work may be needed to define such a role for *PTCSC3*. However, the up-regulation of *PTCSC3* expression in unaffected thyroid tissue of [TT] patients cannot be explained by the action of C/EBPα and C/EBPβ. Instead, the effect of rs944289 genotype on *PTCSC3* expression in thyroid cancer cells likely is linked, at least partially, with the action of these TFs. It is known that C/EBPα and C/EBPβ are expressed in thyroid and suppressed in tumor tissue (http://cgap.nci.nih.gov/cgap.html) (30, 31). C/EBPα modulates (in collaboration with other transcription factors) expression of tissue-specific genes that results in cell proliferation arrest, tissue development, and differentiation (32–36). C/EBPα is a major player in hematopoietic differentiation, and its involvement in hematologic malignancies is very well documented (37, 38). It also has been described as a tumor suppressor in lung and liver tumors (39, 40). The function of C/EBPβ in tumorigenesis is less investigated (41, 42). Our findings show that both C/EBPα and C/EBPβ activate *PTCSC3* promoter activity and that the risk allele significantly reduces the activity generated by p42 C/EBPα and C/EBPβ.

The fact that *PTCSC3* expression is highly thyroid specific suggests that it is involved in thyroid function. Four well-known thyroid-specific genes are involved in hormone synthesis (*TG*, *TPO*, *NIS,* and *TSHR*). In our transfection experiment, the Agilent gene expression array did not show any impact of *PTCSC3* on the expression of these genes. Therefore, thyroid specific genes are unlikely to be the targets of *PTCSC3*. Indeed, the three networks ranked the highest by IPA showed that genes affected by *PTCSC3* possess functions associated with DNA replication, recombination, and repair (network-1), cellular movement, tumor morphology, cell death (network-2), and cellular assembly and tissue morphology (network-3).

We note with interest that in a recent large experiment using genome-wide RNA deep sequencing of multiple tissues, more than 8000 lincRNAs were detected. Among them, *PTCSC3* was studied by computational analysis, and a putative connection with rs944289 as well as the possible involvement of C/EBPα were predicted (23).

In conclusion, our data identify a thyroid-specific lincRNA gene (*PTCSC3*) located in a linkage disequilibrium block with a GWAS-derived SNP (rs944289). We show here that the risk allele decreases promoter activation by weakening the binding affinity of the p42 C/EBPα and C/EBPβ transcription factors. *PTCSC3* expression is significantly down-regulated in tumor compared with unaffected thyroid tissue, and the risk allele is associated with significantly stronger suppression of *PTCSC3*. The restoration of *PTCSC3* expression in PTC cell line affects genes involved in thyroid tumorigenesis and inhibits cell growth. We therefore propose that rs944289 predisposes to PTC by dysregulating the expression of *PTCSC3*, which acts as a tumor-suppressor.

Materials and Methods

A detailed description of materials and methods used can be found in *SI Materials and Methods.*

Thyroid tissue samples. All samples included in this study were collected at The Ohio State University as part of ongoing studies approved by the Institutional Review Board at OSU.

Cell lines. TPC-1 and BCPAP cells were a kind gift from Matthew D. Ringel and Motoyasu Saji (The Ohio State University, Columbus, OH). COS-7 and 293T cells were purchased from ATCC.

In Silico Analysis. To search for the genes and ESTs in the vicinity of rs944289, we used genome browser (http://genome.ucsc.edu/cgi-bin/hgGateway, assembly February 2009, GRCh37/hg19). The potential transcription factor binding sites around the SNP were searched for by using the MATCH program (43).

Real-Time PCR Measurement of *PTCSC3* Expression. SYBR Green real-time PCR system (Applied Biosystems) was used to assess *PTCSC3* expression in PTC patients. The Master mix for each reaction of 10 μL total volume was prepared as follows: 2× SYBR Green Master mix 5 μL, forward primer 200 nM (5′-TCAAACTCCAGGGCTTGAAC-3′), reverse primer 200 nM (5′-ATTACGGCTGGGTC-

TACCT-3′), cDNA 100 ng. For each plate, a dissociation curve was obtained to monitor any additional double stranded DNA. *GAPDH* was used as an internal control and the formula $2^{-\Delta Ct}$, where $\Delta Ct = Ct_{(GENE)} - Ct_{(GAPDH)}$ was used to calculate the relative mRNA level.

RNA Ligase Mediated Rapid Amplification of cDNA Ends. RNA Ligase Mediated Rapid Amplification of cDNA Ends kit (RLM-RACE, Ambion) was used to establish the full structure of CB987890 according to the protocol of the manufacturer. The CB987890 specific primers used in 3′-RLM-RACE were as follows: outer 5′-TGGGACCTGTTGTTTTTCTTG-3′; inner 5′-TCAAACTCCAGGGCTTGAAC-3′. For 5′-RLM-RACE, the CB987890 specific primers were as follows: outer 5′-CATTTTGCCACCATGGTCTA-3′; inner 5′-TCTTCTGCTTGGCCTTTGAC-3′. The Expand Long Template PCR system (Roche) was used for nested PCR reactions for both 5′- and 3′-RLM-RACE, and the TOPO TA kit (Invitrogen) was used to clone nested amplicons into pCR4-TOPO vector. The clones were sequenced using M13 primers.

Northern Blot Analysis. Total RNA was isolated from 293T cells, 293T cells transfected with *PTCSC3* expression vector, and thyroid tissue by using TRIzol solution (Invitrogen). Total RNA (20 μg) was separated on a 1% formaldehyde gel and transferred onto Hybond N membrane (GE Healthcare Life Sciences) and crosslinked (Stratalinker 1800 UV, Stratagene). The membrane was hybridized at 42 °C in UltraHyb Ultrasensitive buffer (Ambion). A 183-bp DNA probe corresponding to 125–307 nucleotides of *PTCSC3* cDNA served as probe. Following overnight hybridization, the membrane was washed in 2xSSC/0.2% SDS at 42 °C.

Constructs. The cDNA of *PTCSC3* was amplified by PCR (forward primer: 5′-gtacggtaccCTCCTTCAGACTTCTCAGTACTC-3′; reverse primer: 5′-tcgactcgagATTGCTACTGTGAGCATAACCTAC-3′), and the amplicons were ligated between Kpn-I and Xho-I sites of the pcDNA3 vector (Invitrogen) to create the expression construct for *PTCSC3*. The construct was confirmed by Sanger sequencing. The promoter region of *PTCSC3* containing rs944289 was amplified by using forward (5′-atcaggtaccGGCAATTGAAGTTCCCAAAA-3′) and reverse (5′-atcactcgagGCCTCCAGACTTGGACTGAG-3′) primers from DNA of homozygous C and homozygous T patients. The amplicons were ligated between Kpn-I and Xho-I sites of the pGL4.24 vector (Promega) and the obtained constructs (C allele: rs944289-C and T allele: rs944289-T) were confirmed by sequencing. C/EBPα (p30 and p42) and C/EBPβ were cloned into pcDNA3-FLAG vector kindly provided by Daniel G. Tenen (Harvard Medical School, Boston, MA).

Luciferase Assay. COS-7 cells were seeded in quadruplicate into 24-well plates, and after 24 h were transfected as shown in Fig. 3 using Lipofectamine 2000 (Invitrogen). The cells were harvested 24 h after transfection using Passive Lysis Buffer (Promega). The promoter activity was determined as *Firefly*/*Renilla* ratio relative to the ratio obtained in cells transfected with the empty vector.

Electrophoretic Mobility Shift Assay. 293T cells were transfected with an empty vector (pcDNA3-FLAG), p30 C/EBPα, p42 C/EBPα or C/EBPβ expression vectors. After 24 h, cells were harvested and nuclear extract was prepared. For the electrophoretic mobility shift assay (EMSA), the double-stranded oligonucleotide probe for the C allele (5′-GGAAAGATAGTCATTGCAGATTTGTAATA-3′) was labeled by filling in the ends with [α-P^{32}]-dCTP by Klenow. The nuclear extracts were incubated with radiolabeled oligonucleotide on ice for 20 min. For the supershift, 1 μL of polyclonal anti-C/EBP (α or β) antibody (Santa Cruz) was added to the binding reaction mixture. Binding reaction products were resolved on a 4% (wt/vol) nondenaturing polyacrylamide gel and electrophoresed at 150 V at 4 °C for 2 h.

***PTCSC3* cDNA resequencing.** RNA from unaffected thyroid and tumor tissue (extracted by TRIzol solution) was DNase-1 treated (Ambion), and High Capacity Reverse transcriptase kit (Applied Biosystems) was used to obtain cDNA. After amplification (forward primer: 5′-AAAAACTCCTTCAGACTTCTCAGT-3′; reverse primer: 5′-GTCCCAGTCCCAAAACTGAA-3′), the PCR amplicons were Sanger sequenced.

Microarray Hybridization Following Transfection with *PTCSC3*. TPC-1 cells (with no endogenous expression of *PTCSC3*) were plated in a 12-well dish and transfected in quadruplicate with 50 ng *PTCSC3* expression construct, and with 50 ng empty vector (pcDNA3) as control using 2 μL Lipofectamine 2000 reagent (Invitrogen). At 24 h after transfection total RNA was extracted (TRIzol reagent, Invitrogen) and DNase-1 treated (Ambion). SurePrint G3 Human Gene Expression 8 × 60,000 Arrays (AMADID 028004; Agilent Technologies) were used to assess gene expression according to manufacturer's protocol (Agilent Technologies).

Cell Growth Assay. TPC-1 and BCPAP cells were seeded into 100-mm plates (5×10^5 cells) and the next day transfected with 5 μg of empty vector (pcDNA3) or *PTCSC3* construct using 12 μL Lipofectamine 2000 (Invitrogen). After 12 h, the cells were seeded in six replicates in 96-well plates (10^3 cells/well). Subsequently, 24 h, 48 h, and 72 h after transfection, 10 μL alamarBlue reagent (Invitrogen) was added to the cells, and after 1 h of incubation the fluorescence intensity was measured by fluorescence microplate reader (SpectraMax M2, Molecular Devices).

ACKNOWLEDGMENTS. The authors thank Stephan Tanner and Agnieszka Bronisz for helpful technical advice, Matthew D. Ringel and Motoyasu Saji for providing the TPC-1 and BCPAP cell lines, Daniel G. Tenen for providing the C/EBP constructs, and Krystian Jazdzewski for critical reading of the manuscript. This work was supported by National Cancer Institute Grants P30CA16058 and P01CA124570.

1. Chen AY, Jemal A, Ward EM (2009) Increasing incidence of differentiated thyroid cancer in the United States, 1988-2005. *Cancer* 115:3801–3807.
2. Howlader NNA, et al. (2010) SEER Cancer Statistics Review, 1975-2008, National Cancer Institute. Bethesda, MD, Available at http://seer.cancer.gov/csr/1975_2008/. Accessed January 22, 2012.
3. Schneider AB, Sarne DH (2005) Long-term risks for thyroid cancer and other neoplasms after exposure to radiation. *Nat Clin Pract Endocrinol Metab* 1:82–91.
4. Goldgar DE, Easton DF, Cannon-Albright LA, Skolnick MH (1994) Systematic population-based assessment of cancer risk in first-degree relatives of cancer probands. *J Natl Cancer Inst* 86:1600–1608.
5. Risch N (2001) The genetic epidemiology of cancer: Interpreting family and twin studies and their implications for molecular genetic approaches. *Cancer Epidemiol Biomarkers Prev* 10:733–741.
6. Dong C, Hemminki K (2001) Modification of cancer risks in offspring by sibling and parental cancers from 2,112,616 nuclear families. *Int J Cancer* 92:144–150.
7. Ito Y, et al. (2009) Biological behavior and prognosis of familial papillary thyroid carcinoma. *Surgery* 145:100–105.
8. Uchino S, et al. (2002) Familial nonmedullary thyroid carcinoma characterized by multifocality and a high recurrence rate in a large study population. *World J Surg* 26: 897–902.
9. de la Chapelle A, Jazdzewski K (2011) MicroRNAs in thyroid cancer. *J Clin Endocrinol Metab* 96:3326–3336.
10. Manolio TA, et al. (2009) Finding the missing heritability of complex diseases. *Nature* 461:747–753.
11. Gudmundsson J, et al. (2009) Common variants on 9q22.33 and 14q13.3 predispose to thyroid cancer in European populations. *Nat Genet* 41:460–464.
12. Takahashi M, et al. (2010) The FOXE1 locus is a major genetic determinant for radiation-related thyroid carcinoma in Chernobyl. *Hum Mol Genet* 19:2516–2523.
13. Gudmundsson J, et al. (2012) Discovery of common variants associated with low TSH levels and thyroid cancer risk. *Nat Genet* 44:319–322.
14. Matsuse M, et al. (2011) The FOXE1 and NKX2-1 loci are associated with susceptibility to papillary thyroid carcinoma in the Japanese population. *J Med Genet* 48:645–648.
15. Jones AM, et al.; TCUKIN Consortium (2012) Thyroid cancer susceptibility polymorphisms: Confirmation of loci on chromosomes 9q22 and 14q13, validation of a recessive 8q24 locus and failure to replicate a locus on 5q24. *J Med Genet* 49: 158–163.
16. Fujita PA, et al. (2011) The UCSC Genome Browser database: Update 2011. *Nucleic Acids Res* 39(Database issue):D876–D882.
17. Mariner PD, et al. (2008) Human Alu RNA is a modular transacting repressor of mRNA transcription during heat shock. *Mol Cell* 29:499–509.
18. Ponicsan SL, Kugel JF, Goodrich JA (2010) Genomic gems: SINE RNAs regulate mRNA production. *Curr Opin Genet Dev* 20:149–155.
19. Freedman ML, et al. (2011) Principles for the post-GWAS functional characterization of cancer risk loci. *Nat Genet* 43:513–518.
20. Donnelly P (2008) Progress and challenges in genome-wide association studies in humans. *Nature* 456:728–731.
21. Hindorff LA, et al. (2009) Potential etiologic and functional implications of genome-wide association loci for human diseases and traits. *Proc Natl Acad Sci USA* 106: 9362–9367.
22. Prensner JR, et al. (2011) Transcriptome sequencing across a prostate cancer cohort identifies PCAT-1, an unannotated lincRNA implicated in disease progression. *Nat Biotechnol* 29:742–749.
23. Cabili MN, et al. (2011) Integrative annotation of human large intergenic noncoding RNAs reveals global properties and specific subclasses. *Genes Dev* 25:1915–1927.
24. Morley M, et al. (2004) Genetic analysis of genome-wide variation in human gene expression. *Nature* 430:743–747.
25. Göring HH, et al. (2007) Discovery of expression QTLs using large-scale transcriptional profiling in human lymphocytes. *Nat Genet* 39:1208–1216.
26. Stranger BE, et al. (2007) Population genomics of human gene expression. *Nat Genet* 39:1217–1224.

27. van Staveren WC, et al. (2007) Human thyroid tumor cell lines derived from different tumor types present a common dedifferentiated phenotype. *Cancer Res* 67: 8113–8120.
28. Pelosi G, et al. (2010) Dual role of RASSF1 as a tumor suppressor and an oncogene in neuroendocrine tumors of the lung. *Anticancer Res* 30:4269–4281.
29. Yang L, Han Y, Suarez Saiz F, Minden MD (2007) A tumor suppressor and oncogene: The WT1 story. *Leukemia* 21:868–876.
30. Pomérance M, Mockey M, Young J, Quillard J, Blondeau JP (2005) Expression, hormonal regulation, and subcellular localization of CCAAT/enhancer-binding protein-beta in rat and human thyrocytes. *Thyroid* 15:197–204.
31. Akagi T, et al. (2008) Induction of sodium iodide symporter gene and molecular characterisation of HNF3 beta/FoxA2, TTF-1 and C/EBP beta in thyroid carcinoma cells. *Br J Cancer* 99:781–788.
32. Flodby P, Barlow C, Kylefjord H, Ahrlund-Richter L, Xanthopoulos KG (1996) Increased hepatic cell proliferation and lung abnormalities in mice deficient in CCAAT/enhancer binding protein alpha. *J Biol Chem* 271:24753–24760.
33. Sugahara K, et al. (2001) Mice lacking CCAAt/enhancer-binding protein-alpha show hyperproliferation of alveolar type II cells and increased surfactant protein mRNAs. *Cell Tissue Res* 306:57–63.
34. Tontonoz P, Hu E, Spiegelman BM (1994) Stimulation of adipogenesis in fibroblasts by PPAR gamma 2, a lipid-activated transcription factor. *Cell* 79:1147–1156.
35. McNagny KM, Sieweke MH, Döderlein G, Graf T, Nerlov C (1998) Regulation of eosinophil-specific gene expression by a C/EBP-Ets complex and GATA-1. *EMBO J* 17:3669–3680.
36. Cassel TN, Suske G, Nord M (2000) C/EBP alpha and TTF-1 synergistically transactivate the Clara cell secretory protein gene. *Ann N Y Acad Sci* 923:300–302.
37. Pabst T, et al. (2001) Dominant-negative mutations of CEBPA, encoding CCAAT/enhancer binding protein-alpha (C/EBPalpha), in acute myeloid leukemia. *Nat Genet* 27: 263–270.
38. Tenen DG (2003) Disruption of differentiation in human cancer: AML shows the way. *Nat Rev Cancer* 3:89–101.
39. Halmos B, et al. (2002) Down-regulation and antiproliferative role of C/EBPalpha in lung cancer. *Cancer Res* 62:528–534.
40. Tan EH, et al. (2005) CCAAT/enhancer binding protein alpha knock-in mice exhibit early liver glycogen storage and reduced susceptibility to hepatocellular carcinoma. *Cancer Res* 65:10330–10337.
41. Armstrong DA, Phelps LN, Vincenti MP (2009) CCAAT enhancer binding protein-beta regulates matrix metalloproteinase-1 expression in interleukin-1beta-stimulated A549 lung carcinoma cells. *Mol Cancer Res* 7:1517–1524.
42. Zahnow CA (2009) CCAAT/enhancer-binding protein beta: Its role in breast cancer and associations with receptor tyrosine kinases. *Expert Rev Mol Med* 11:e12.
43. Kel AE, et al. (2003) MATCH: A tool for searching transcription factor binding sites in DNA sequences. *Nucleic Acids Res* 31:3576–3579.